Lasers in Manufacturing Conference 2015

Laser-GMA-Hybrid Welding of high strength multi-material joints

Felix Möller[a]*, Helge Kügler[a], Sven-F. Goecke[b]

[a]*BIAS – Bremer Institut für angewandte Strahltechnik GmbH, Klagenfurter Straße 2, 28359 Bremen*
[b]*Fachhochschule Brandenburg, Magdeburger Strße 50, 14770 Brandenburg an der Havel*

Abstract

A particular challenge for welding 22MnB5 and DP800 are the coatings of each steel sheet. As a prevention of oxidation during press-hardening 22MnB5 sheets are protected with an aluminum silicon coating. The dual phase steel DP800 is zinc coated in many cases. In this described case the steel sheets are hot-dip galvanized. The evaporation temperature of zinc is below the melting temperature of steel. For that reason a zinc degassing gap between the sheets is necessary for welding in overlap configuration.
At BIAS a laser-GMA-hybrid welding process was established for welding 22MnB5 to DP800. With this process combination weld seams reach a strength exceeding the strength of the heat affected DP800. Tensile tests prove yield strength of 800 N/mm² with failure location in the heat affected zone of DP800.
The laser beam was oscillated 0.7 mm transverse to the feed direction with a frequency of 200 Hz. A feed rate of 3 m/min was realized. The laser beam was able to vaporize zinc 5 mm ahead of the GMA-process which was carried out with a wire feed rate of 14 m/min. For this hybrid welding process a 1 mm thick G3Si1 wire was used.
Occurrence of pores and spatters could be avoided by a gap of 0.4 mm between overlapping sheets. The aluminum silicon coating of 22MnB5 accumulates at the seam tip.

Keywords: Macro Processing; Welding; Laser; GMA; Hybrid; DP800; 22MnB5

* Felix Möller: Tel.: +49 421 218 58035; fax: +49 421 218 58063.
E-mail address: moeller@bias.de.

1. Introduction

Lightweight design for automotive industry is required in order to fulfill environmental protection goals. A new approach of lightweight constructions deals with high strength steel. Especially presshardened steel sheets gain importance in the sector. These new ultra high strength alloys, like 22MnB5, are the material of modern hot formed structural elements, like the B-pillar. Because of its high strength wall thicknesses can be reduced and material and weight is saved. According to Göschel et al. [Gös11], presshardened steels reduces cycle time by higher process efficiency and less process steps. New alloys need appropriate joining concepts. According to Larsson et al. [Lar09] there is a special need for welding of presshardened steels by automotive industry. Kim et al. [Kim11] carried out investigations on weldability of 22MnB5.

Presshardened steels are coated with AlSi in order to prevent oxidation during manufacturing. Analyses of weld seams show a negative influence of this coating. Aluminum and silicon form intermetallic phases along the fusion line. Joint strength especially for dynamic load is significantly weakened as investigations of Kim et al. [Kim11] proof. This weakening is mainly caused by agglomeration of the coating at the seam solidification line. Intermetallic phases occur due to the contact of steel and aluminum and therefore induced diffusion processes. Hybrid welding combining gas metal arc welding (GMAW) and laser beam welding is already well known in industrial applications. Advantages of combining these processes were investigated by Cui [Cui91]. Increased welding speed and penetration depth compared to single process GMAW are possible. Regarding a laser beam welding, process combination achieve higher gap bridgeability according to Bagger and Olsen [Bag05]. Aalderink et al. [Aal07] confirm improved gap bridgeability for hybrid welding compared to regular laser beam welding. It is shown that a hybrid laser GMA welding is capable of bridging a 1 mm gap in case of 2.1 mm aluminum sheets. Cassalino et al. [Cas13] investigated hybrid welding of aluminum. Their results show that laser leading configuration achieves deeper penetration and higher process velocity than with arc leading configuration. Amongst others, these advantages are used for several welding operations on different materials. Verwimp and Gedopt [Ver07] were using this set-up for welding aluminum. Welding steel by Grünenwald et al. [Grü10] and even welding of multi-material joints of steel and aluminum by Walter et al. [Wal08] were applied with this configuration.

Positive effect of combining laser and arc welding is explained by Cui [Cui91] with the laser induced plasma. According to this work, the laser beam has stabilizing influence on the arc welding process. Stute et al. [Stu07] proofed this effect even with very low laser energy input of a few hundred watts. On the other hand, Rippl [Rip08] used hybrid welding process with multi kilowatt lasers which allow T-joint welding of 15 mm thick steel sheets without any weld preparation.

2. Experimental

2.1. Material

Table 1 – chemical composition of used materials. General information of EWM (2014) and ThyssenKrupp Steel (2014)

Material	C	Si	Mn	P	S	Al (min)	Nb	Ti	Cr+Mo	B
DP800	0.18	0.24	1.7	0.014	0.004	0.04	0.05	0.05	0.56	0.0001
22MnB5	0.25	0.4	1.4	0.025	0.01	0.015	0.1	0.05	0.5	0.005
G3Si1	0.08	0.9	1.5	0.015	0.012	-	-	-		-
	values in weight percent									

Möller 2015 BIAS ID 140976

For this results ultra-high strength 22MnB5 and DP800 steel sheets with thickness of 1.5 mm were welded. For the GMA welding G3Si1 (1.5125) filler wire was used with a diameter of 1 mm.

2.2. Set-Up

Investigations on laser GMA hybrid welding of 22MnB5 steel sheets and zinc coated DP800 in overlap configuration were carried out using an IPG YLR 1000 SM single mode fiber laser and an EWM alphaQ 552 GMAW source. Additionally a Phoenix drive wire feeder and an Abicor Binzel WH 535 Hybrid GMAW torch were used. This power supply and GMAW peripheries provide pulsed arc welding for the hybrid process.

The single mode laser provides up to 1 kW output power using a fiber with a diameter of 15 µm. For these shown experiments an optical set-up with a collimation length of 160 mm and a focal length of 200 mm were installed. A spot size of 24.5 µm in focal plane was measured with a Primes MicroSpotMonitor. Welding was carried out with the laser beam focused on the bottom sheet surface. Additional laser beam oscillation was realized with a DC-ILV-Scanner by Co. Arlt. This system enables oscillating the laser beam transverse to the welding direction.

In figure 1 principle of the process arrangement is demonstrated. Fillet welds on steel sheets with an overlap of 16 mm according to SEP 1220 [SEP11] were welded. A fillet weld angle of $\alpha = 30°$ is necessary. Laser beam irradiation was kept under an angle of $\beta_{laser} = 20°$ whereas GMAW torch had an inclination angle of $\beta_{torch} = 15°$. Laser beam oscillation was performed with a constant frequency of $f_S = 200$ Hz and an amplitude of $2A_S = 0.7$ mm transverse to the welding direction.

Positioning of the laser beam and the GMAW torch were kept constant throughout these experiments. Welding velocity and laser beam oscillation amplitude and frequency were also constant. Values of these parameters are given in table 1. A shielding gas composed of 82 % argon and 18 % CO2 was used with a flow rate of 15 l/min for these experiments.

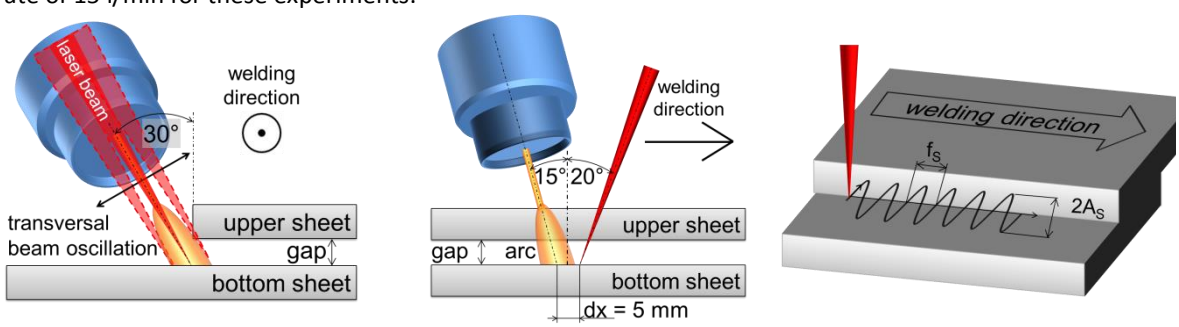

Möller 2015

BIAS ID 150844

Figure 1 – illustrations for process parameters [Küg14]

Welds with a constant gap were realized. Therefore, five spacers were placed between the sheets. This guarantees constant gap conditions over the whole weld seam length and simultaneously does not influence heat conduction too much.

2.3. Method

A variation of the gap sizes was investigated. Gap sizes were set 0.4 mm and 0.6 mm. Subsequently, specimens were analyzed by cross sections and tensile testing. Table 2 presents the parameters which were kept constant during the investigations.

Table 2 – process parameters

parameter		unit	value
Laser power	P_L	kW	1
Focus height	f_z	mm	0
Electrode stickout		mm	18
Arc voltage	U	V	~ 30
Voltage correction	ΔU	V	+ 2
Arc trim		%	+ 10
Arc polarity			DCEP
Torch angle	β_{torch}	°	20

parameter		unit	value
Process velocity	v_p	m/min	3
Hybrid process movement	d_y	mm	0
Fillet weld angle	α	°	30
Laser beam inclination angle	β_{laser}	°	15
Laser beam oscillation frequency	f_S	Hz	200
Laser-GMAW-distance	d_x	mm	5
Laser beam oscillation amplitude	$2A_S$	mm	0.7

Möller 2015 BIAS ID 141514

3. Results and Discussion

3.1. Welding behavior

The most challenging task for thermal welding of zinc coated steel is the evaporating zinc which causes pores, spatters and other welding defects in the joint. In figure 2 typical joint defects are shown by using zero gap configurations. The zinc cannot evaporate so that the vapor influences the flow behavior of the melt pool. A lack of melt on the upper sheet occurs. Therefore, the seam is insufficient for transmissions of forces. Moreover, a higher amount of welding fume deposit on the steel surface can be observed.

Arc torch	Abicor Binzel WH 535
Arc source	EWM alphaQ 552
Laser	IPG YLR 1000 SM
Wire	G3Si1 (Ø1.0 mm)
Wire speed	9 m/min
Laser power	1 kW
Process speed	3 m/min
Gap	0 mm

Möller 2015 BIAS ID 151117

Figure 2: Overlap welded material mix DP800 to 22MnB5

Therefore, two challenges can be defined. First the zinc coating which have to be removed or even evaporated in the joining zone and secondly the Al-Si coating of 22MnB5 which also can cause welding defects due to the formation of intermetallic phases.

In figure 3 a welded steel material mix with the zinc coated DP800 as upper sheet is shown.

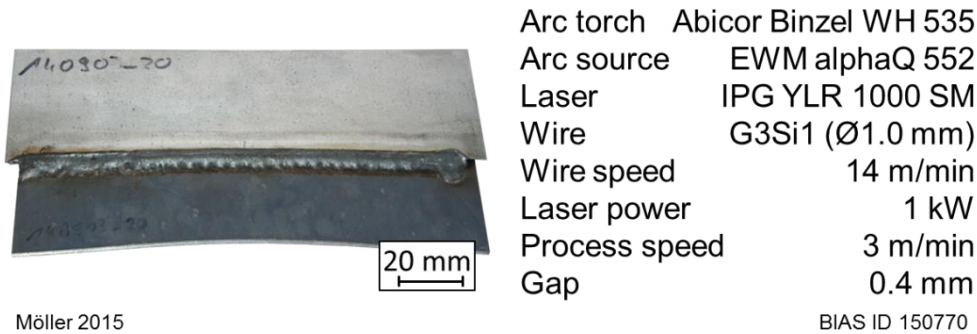

Figure 3: Overlap welded material mix DP800 to 22MnB5

By using the developed joining process set-up the positioning of the processes to each other can be varied. Thus, it is possible to remove the zinc layer as well as melting the Al-Si coating in front of arc process with the preparatory laser beam. Figure 2 demonstrates a defect free joining using a gap of 0.4 mm. The zinc can be evaporated through the gap. Furthermore, the preheated or even melted surface stabilizes the arc. The joining speed can be increased up to 3 m/min in this configuration.

3.2. Metallography

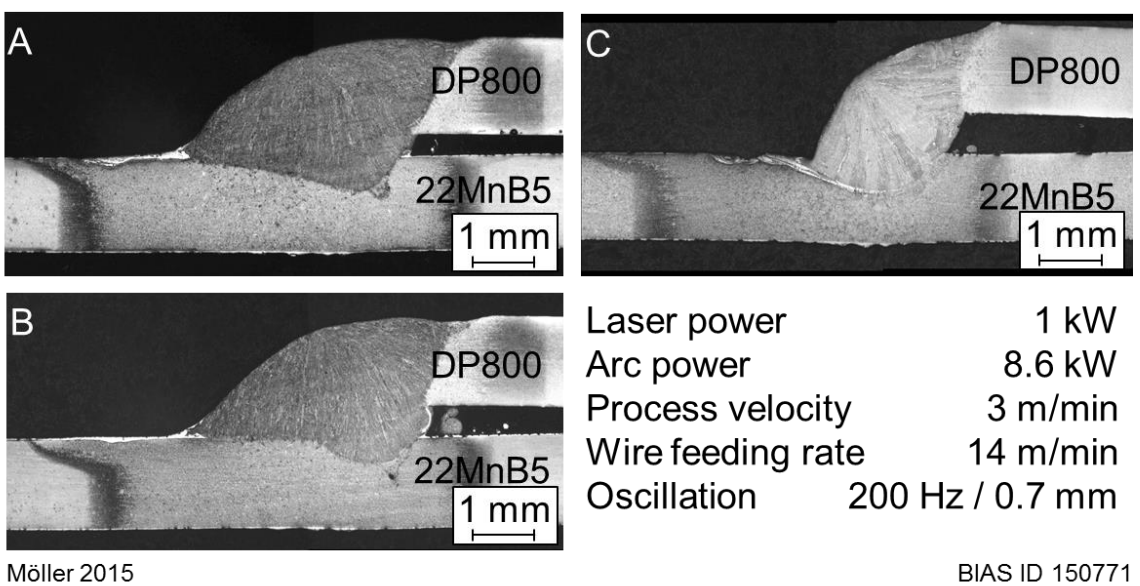

Figure 4: Cross sections of material mix with 0.4 mm gap size (A; B) and 0.6 mm gap size (C)

The joints were characterized using cross sections. Figure 4 demonstrates typical joint appearances. The joints are free of pores. Furthermore, no other welding defects like cracks or inclusions occur. Moreover, figure 4 also presents the influence of the gap size between sheets. As described above a gap is necessary for evaporating zinc to realize a defect free joint. By using a 0.4 mm gap the melt pool has a width of

4.55 mm and a penetration depth of 0.5 mm. For the specimens A and B the same parameters were used to address the reproducibility. The critical crack length, which is the minimum seam section length, is quite similar to the sheet thickness. By adjusting a gap of 0.6 mm the wetting length of the joint is decreased significantly to 2.5 mm. A penetration depth of 0.75 mm can be reached which is an increase of 50 % compared to the 0.4 mm gap.

In front of the melt pool an agglomeration of the AlSi coating can be observed. This effect is also described in the state of the art. The coating was melted by the process and displaced by the filler material. Afterwards the AlSi coating components in the melt are agglomerated at the tip of the weld. A negative aspect of this agglomeration is that cracks can be initiated which results in a failure of the joint.

To get a more detailed overview micro CT was carried out at BIAS. Figure 5 shows a characteristic layer of the welded specimen. Sectional B demonstrates a longitudinal cross section of the weld. In welding direction specimen shows waviness based on meld pool dynamics resulting from high process velocity. No pores or cracks could be detected over the whole seam length.

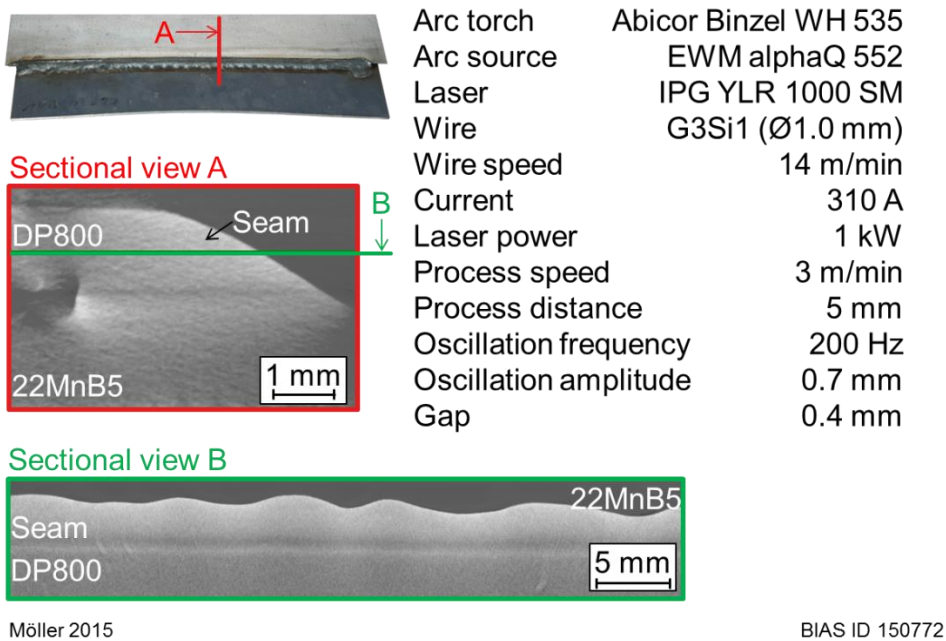

Figure 5: Computed tomography of a welded specimen

3.3. Mechanical properties

Beside metallographic aspects tensile test were carried out to analyze the tensile strength depending on position in the specimen. The specimens were prepared according to SEP 1220. Thus, the results can be compared with other joining technologies. In figure 6 the results of the tensile tests are given. At the beginning of the joint smaller gaps can reach much higher tensile strength. This problem was based on an inconstant process at the start. At a position of 130 mm all specimens reach similar values of approximately 800 N/mm². The effects point out high process tolerance concerning gaps. At the weld seam end lower tensile strength is achieved.

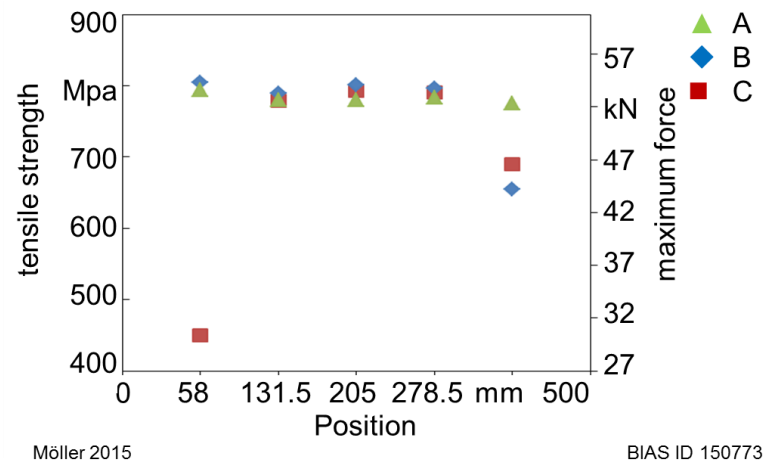

Figure 6: Results of tensile tests

3.4. Surface analysis

In order to analyze the surface conditions after welding specimens were analyzed by EDX. In figure 7 results for the elements zinc and oxygen are presented. Focusing on areas close to the melt pool both elements can be detected. Directly beside the melted area oxygen is dominating the surface. Zinc layer was evaporated by the welding process. Subsequently after welding the area of evaporated zinc is oxidized by environmental atmosphere. By increasing the distance to the melt pool the surface is still coated by zinc.

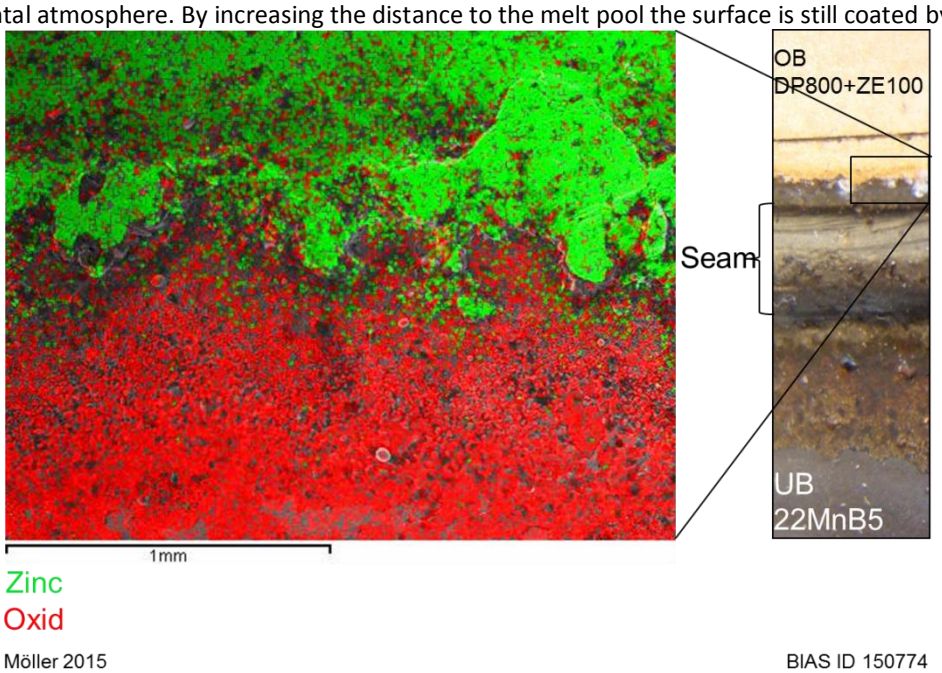

Figure 7: EDX of upper sheet top surface after welding

4. Conclusion

Joining material mixes of different steels is still challenging. By using a combination of laser and arc processes a control of the zinc evaporation is achieved and defect free seams can be welded. This can be achieved by using joining gaps. Thus, the arc process is stable and is not influenced by evaporating zinc. Furthermore, high process velocity and gap tolerances can be achieved. Additionally, state of the art findings that a gap is necessary for thermal joining of zinc coated steel sheets is approved also for a combination of DP800 and 22MnB5+AS.

Acknowledgements

The IGF project No. 17585 BG (P 919) of the FOSTA – Research Association for Steel application was supported by the Arbeitsgemeinschaft industrieller Forschungsvereinigungen e.V. (AiF) under the program for the promotion of industrial research by the Federal Ministry of Economics and Technology based on a decision by the German Bundestag. This support is greatly acknowledged.

References

Bagger, C., Olsen, F.O., 2005. Review of laser hybrid welding. In: Journal Of Laser Applications, volume 17, number 1, Feburary 2005, Laser Institute of America

Casalino, G., Campanelli, S.L., Dal Maso, U., Ludovico, A.D., 2013. Arc leading versus laser leading in the hybrid welding of aluminium alloy using a fiber laser. In: Procedia CIRP 12 (2013), 151-156

Cui, H., 1991. Untersuchung der Wechselwirkung zwischen Schweißlichtbogen und fokussiertem Laserstrahl und der Anwendungsmöglichkeiten kombinierter Laser-Lichtbogentechnik. Fakultät für Maschinenbau und Elektrotechnik der Technischen Universität Carolo-Wilhelmina Braunschweig. Dissertation

Göschel, A., Sterzing, A., Schönherr, J., 2011. Balancing procedure for energy and material flows in sheet metal forming. In: CIRP Journal of Manufacturing Science and Technology 4, 170-179.

Grünenwald, S., Seefeld, T., Vollertsen, F., Kocak, M., 2010. Solutions for joining pipe steels using laser-GMA-hybrid welding processes. Laser Assisted Net shape Engineering 6 (LANE 2010), In: Physics Procedia 5 (2010), 77–87

Kim, C., Kang, M. J., Park, Y. D., 2011. Laser welding of Al-Si coated hot stamping steel. In: International Conference on the Mechanical Behavior of Materials (ICM11), Procedia Engineering 10 (2011), 2226-2231.

Larsson, J.K., Lundgren, J., Asbjornsson, E., Andersson, H., 2009. Extensive introduction of ultra high strength steels sets new standards for welding in the body shop. In: Welding in the World 53, 5/6, 4-14

Möller, F., Mittelstädt, C., Kötschau, S., Thomy, C., Goecke, S.-F., Vollertsen F., 2013. Effect of process parameters on joint properties in laser GMA hybrid welding of thin-sheet fillet welds on 22MnB5. In: IIW 2013 Annual Assembly Com. XVII, Essen (2013) IIW-Doc. XII-2129-13; IV- 1138-13 (online)

Möller, F.; Kügler, H.; Kötschau, S.; Geier, A.; Goecke, S.-F.: Gap bridging ability in laser GMA hybrid welding of thin 22MnB5 sheets. 8th International Conference on Laser Assisted Net Shape Engineering LANE 2014 In: Physics Procedia. Volume 56 (2014) 620-629

Kügler, H.; Möller, F.; Kötschau, S.; Geier, A.; Goecke, S. F.; Vollertsen. F.: Bridgeability of increasing gap in laser GMA hybrid welding of 22MnB5. In: IIW Annual Assembly 2014 Com. XII. Seoul/Korea (2014) IIW-Doc. XII-2169-14 (online)

N.N., 2014. EWM product data sheet "Drahtelektrode SW 70S G3". G 42 3M G3Si1 (1.5125 DIN EN 14341-A)

N.N., 2014. ThyssenKrupp Steel AG: Mangan-Bor-Stähle MBW. Product information sheet from March 2014; Duisburg, Germany

N.N.: Stahl-Eisen-Prüfblatt (SEP) 1220 – Testing and Documentation Guideline for the Joinability of thin sheet of steel. Verlag Stahleisen GmbH, August 2011

Rippl, P., 2008. Anwendungsbeispiele für die Laser-Hybrid-Technik konventionell und mit Lasern geringer Leistung. In: Strahltechnik Band 36, 107-117, BIAS Verlag, Bremen

Stute, U., Kling, R., Hermsdorf , J., 2007. Interaction between Electrical Arc and Nd: YAG Laser Radiation. In: Annals of the CIRP Vol. 56/1/2007, 197-200

Verwimp, J., Gedopt, J., 2007. Hybrid Laser Welding and Friction Stir Welding Applied to 6056 Aluminium Alloy. In: Proceeding of the APT'07: International Conference on Applied Production Technology, 109-122 , BIAS Verlag, Bremen

Walther, R., Thomy, C., Möller, F., Vollertsen, F., 2008. Thermisches Fügen von Mischverbindungen. In: Strahltechnik Band 36, 37-49, BIAS Verlag, Bremen